On Source Coding, Channel Coding and Spreading Tradeoffs in a DS-CDMA System Operating Over Frequency Selective Fading Channels With Narrowband Interference

Ramesh Annavajjala, *Student Member, IEEE*, Pamela C. Cosman, *Senior Member, IEEE*, and Laurence B. Milstein, *Fellow, IEEE*

***Abstract*—For a fixed total bandwidth expansion factor, we consider the problem of optimal bandwidth allocation among the source coder, the channel coder, and the spread-spectrum unit for a direct-sequence code-division multiple-access system operating over a frequency-selective fading channel with narrowband interference. Assuming a Gaussian source with the optimum scalar quantizer, and a binary convolutional code with soft-decision decoding, and further assuming that the self-interference is negligible, we obtain both a lower and an upper bound on the end-to-end average source distortion. The joint three-way constrained optimization of the source code rate, the channel code rate, and the spreading factor can be simplified into an unconstrained optimization problem over two variables. Upon fixing the channel code rate, we show that both upper and lower bound-based distortion functions are convex functions of the source code rate. Because an explicit solution for the optimum source code rate, i.e., one that minimizes the average distortion, is difficult to obtain, computer-based search techniques are employed. Numerical results are presented for the optimum source code rate and spreading factor, parameterized by the channel code rate and code constraint length. The optimal bandwidth allocation, in general, depends on the system and the channel conditions, such as the total number of active users, the average jammer-to-signal power ratio, and the number of resolved multipath components together with their power delay profile.**

***Index Terms*—Bandwidth constraint, channel coding, cross-layer optimization, source coding, spread spectrum.**

I. Introduction

IT IS WELL KNOWN that efficient channel coding together with the processing gain inherent in the use of spread-spectrum enables a direct-sequence code-division multiple-access (DS-CDMA) system to successfully combat the effects of multipath distortion, multiple access interference (MAI), and intentional/unintentional narrowband interference (NBI) [1]–[3]. However, for a fixed spread bandwidth, transmission of high quality source information competes for the available bandwidth with channel coding and spreading. This motivates us to study the tradeoffs involved among source coding, channel coding, and spreading in a DS-CDMA system.

We first briefly review the related previous work. In [4] and [5], an information theoretic approach is taken to investigate the tradeoffs between source and channel coding. In [6] and [7], the tradeoff between coding and spreading is investigated for a spread-spectrum system. Using system level simulations, in [8], Zhao *et al.* studied the problem of optimal bandwidth allocation among source coder, channel coder, and spread-spectrum modulator for progressive transmission of images over frequency-selective fading channels with MAI. Recently, in [9], an analysis was presented for the optimal bandwidth allocation on additive white Gaussian noise (AWGN) and flat Rayleigh-fading CDMA channels for both block coding with hard-decision decoding and convolutional coding with soft-decision decoding.

In this paper, we extend the analysis of [9] to the case of a frequency-selective fading channel with NBI. We assume a Gaussian source with the optimum scalar quantizer and a binary convolutional code with soft-decision decoding. For the sake of generality, we model the individual multipath components as independent, Nakagami-m distributed random variables with arbitrary fading parameters, and assume that the NBI is a Gaussian distributed partial-band interferer (PBI). Using a standard Gaussian approximation for the MAI, we obtain an upper and a lower bound on the pairwise error probability (PEP) with soft-decision decoding, using which we bound the end-to-end average source distortion. In our analysis, we assume that the self-interference is negligible. As a consequence, our analytical results apply to scenarios such as where the dominant source of interference is due to MAI and/or jamming. We first note that the joint three-way constrained optimization of the source code rate, the channel code rate, and the spreading factor can be simplified into an unconstrained optimization problem over two variables. Upon fixing the channel code rate, we show that both upper and lower bound-based distortion functions are convex functions of the source code rate. An explicit solution for the optimum source code rate, that minimizes the average distortion, is difficult to obtain and requires computer-based search techniques. We note that the analysis of [9], which is valid for both an AWGN channel and a flat Rayleigh-fading channel, can be viewed as a special case of the analysis presented in this paper. Numerical results are given for the optimum source

Manuscript received April 1, 2004; revised January 27, 2005. This work was supported in part by the Office of Naval Research under Grant N00014-03-1-0280.

The authors are with the Department of Electrical and Computer Engineering, University of California, San Diego, La Jolla, CA 92093-0407 USA (e-mail: ramesh@cwc.ucsd.edu; pcosman@ucsd.edu; milstein@ece.ucsd.edu).

Digital Object Identifier 10.1109/JSAC.2005.845416

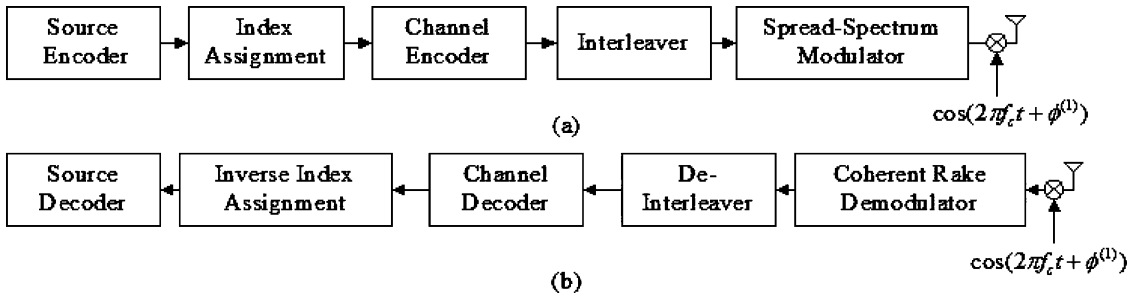

Fig. 1. Block diagram of the transmitter—receiver pair for the desired user. (a) Transmitter. (b) Receiver.

code rate and spreading factor, parameterized by the channel code rate and code constraint length. Results indicate that the optimal bandwidth allocation, in general, depends on the system and the channel conditions, such as the total number of active users, the average jammer-to-signal power ratio (JSR), and the number of resolved multipath components together with their power delay profile.

The rest of this paper is organized as follows. In Section II, we introduce both our system and the channel model, and derive upper and lower bounds on the pairwise error probability with soft-decision decoding. Analysis of the end-to-end average distortion with soft-decision channel decoding is presented in Section III, and the optimum bandwidth allocation problem is detailed in Section IV. Numerical results and discussion are provided in Section V. Finally, we conclude our work in Section VI.

II. System Model

The transmitter-receiver pair for the user-of-interest is shown in Fig. 1. The information source is quantized by the source encoder with a rate of r_s bits per source sample, which are then mapped onto a new bit index of the same length r_s using an index assignment block. While ordinarily the purpose of an index assignment is to permute indices so that small Hamming distance corresponds to close quantization levels, for ease of analysis, as in [9] and [11], we assume a random index assignment with a one-to-one mapping of indices from 0 through $2^{r_s}-1$.

The bit stream at the output of the index assignment block is encoded with a convolutional code of rate r_c, whose output is interleaved, assumed to be ideal, before passing through the spread-spectrum modulator. We now present the mathematical model for the transmitter, the channel, and the receiver.

A. Transmit Signal Model

With K_u simultaneous users in the system, the transmitted signal for the kth user is denoted by $S^{(k)}(t)$, and is expressed in the form

$$S^{(k)}(t) = \sqrt{2P}a^{(k)}(t)d^{(k)}(t)\cos\left(2\pi f_c t + \phi^{(k)}\right) \quad (1)$$

where P is the transmit power, assumed to be common to all the users, f_c is the carrier frequency in Hertz, $\phi^{(k)}$ is the initial phase angle, and $a^{(k)}(t)$ is the spreading code sequence of the kth user, which can be expressed as $a^{(k)}(t) = \sum_{j=-\infty}^{\infty} a_k[j]h_{T_c}(t - jT_c)$, where $a_k[j] \in \{-1,+1\}$, and $h_{\mathcal{T}}(t)$ is a rectangular pulse shape filter with $h_{\mathcal{T}}(t) = 1$ for $0 \le t < \mathcal{T}$, and is zero elsewhere. The data signal of the kth user $d^{(k)}(t)$ is given by $d^{(k)}(t) = \sum_{j=-\infty}^{\infty} d_k[j]h_{T_s}(t - jT_s)$, where $d_k[j] \in \{-1,1\}$ denotes the coded data stream, and T_s is the symbol duration, which is related to the bit duration T_b by $T_s = T_b r_c$ so that the energy-per-bit E_b can be expressed as $E_b = PT_b = PT_s/r_c$. We assume that the spreading sequence $\{a_k[j]\}$ is long enough to be considered as a random binary sequence with period much longer than the symbol duration. The spread factor $\mathcal{S}_F$ of this coded system is defined as $\mathcal{S}_F = T_s/T_c = T_b r_c/T_c$.

B. Channel Model

The channel is assumed to be frequency-selective and is slowly fading over the duration of T_s. The low-pass equivalent impulse response for the kth user is given by

$$h^{(k)}(t) = \sum_{l=0}^{L-1} \alpha_l^{(k)} e^{j\theta_l^{(k)}} \delta\left(t - \tau_l^{(k)}\right) \quad (2)$$

where L is the number of resolved multipaths, which is related to the multipath delay spread T_m and the chip duration T_c by $L = \lfloor T_m/T_c \rfloor + 1$, where $\lfloor x \rfloor$ denotes the largest integer that is less than or equal to x. The parameter $\alpha_l^{(k)}$ is the random amplitude fade on the lth path, which is assumed to be Nakagami-m distributed with the probability density function (pdf) [12]

$$f_{\alpha_l^{(k)}}(x) = \frac{2m_l^{m_l}}{\Omega_l^{m_l}\Gamma(m_l)} \exp\left(-\frac{m_l x^2}{\Omega_l}\right) x^{2m_l-1}, \quad x \ge 0 \quad (3)$$

where $m_l \ge 0.5$ is the Nakagami parameter, also known as the fading severity index, and $\Omega_l = E[(\alpha_l^{(k)})^2]$ is the average fading power on the lth path, which is assumed to be independent of the user index k. We note that the pdf expression of (3) allows us to investigate the bandwidth tradeoff problem on generalized wideband fading channels with variable severity of individual resolvable multipaths. For simplicity, similar to [13] and [14], we assume that the random phase $\theta_l^{(k)}$ is independent of $\alpha_l^{(k)}$, and is uniformly distributed over $[0, 2\pi)$. The random variable $\tau_l^{(k)}$ denotes propagation delay on the lth path, and is assumed to be uniformly distributed in $[0, T_c)$.

In addition to the above described multipath, the transmitted signal is also affected by a narrowband jammer, which, in this paper, is modeled as a Gaussian-distributed PBI, $J(t)$, with a power spectral density

$$S_J(f) = \begin{cases} \frac{\eta_J}{2}, & \text{for } f_c - \frac{W_J}{2} \le |f| \le f_c + \frac{W_J}{2} \\ 0, & \text{otherwise} \end{cases} \quad (4)$$

where η_J and W_J are the one-sided power spectral density and the bandwidth of the PBI, respectively. Finally, the average power of the jammer is denoted by $\mathcal{N}_J$, and is given by $\mathcal{N}_J = \eta_J W_J$.

C. Receiver Model

Without loss of generality, we assume that the first user (i.e., $k=1$) is the user-of-interest. With this, the received signal after passing through the frequency-selective fading channel with a PBI can be expressed as

$$r(t)=\sum_{k=1}^{K_u}\sqrt{2P}\sum_{l=0}^{L-1}\alpha_l^{(k)}a^{(k)}\left(t-\tau_l^{(k)}\right)d^{(k)}\left(t-\tau_l^{(k)}\right)\times\cos\left(2\pi f_c t+\psi_l^{(k)}\right)+n(t)+J(t) \quad (5)$$

where $\psi_l^{(k)}=-2\pi f_c\tau_l^{(k)}+\theta_l^{(k)}+\phi^{(k)}$ is the effective phase on the lth path of the kth user, and $n(t)$ is zero-mean AWGN with two-sided power spectral density of $N_0/2$.

We assume that the code acquisition for the desired user is successful, so that the matched filter on the first finger of the RAKE receiver is synchronized to the last path of the desired user. We also assume perfect knowledge of the desired user's fade coefficients $\{\alpha_l^{(1)}\}$. With this, the output of the RAKE receiver during the nth code symbol is given by [13]

$$\begin{aligned}Z_n&=\sum_{l=0}^{L-1}\int_{lT_c}^{lT_c+T_s}r(t)\alpha_l^{(1)}[n]a^{(1)}(t-lT_c)\cos\left(w_c t+\psi_l^{(1)}[n]\right)dt\\&=\sum_{l=0}^{L-1}\left(D_l[n]+I_l^{\mathrm{SI}}[n]+I_l^{\mathrm{MAI}}[n]+N_l[n]+J_l[n]\right)\end{aligned} \quad (6)$$

where the subscript l and the index n denote, respectively, the path index and the symbol index, and the other terms of (6) are defined as follows: 1) $D_l[n]$ is the component of the test statistic due to the desired user; 2) I_l^{SI} is the self interference of user 1, due to the nonimpulsive nature of the autocorrelation function of the spreading code; 3) $I_l^{\mathrm{MAI}}[n]$ is the MAI due to the other K_u-1 users; 4) $N_l[n]$ is the contribution due to the AWGN; and 4) $J_l[n]$ is the contribution made by the jammer. Following the analysis of [13], one can show that the terms $D_l[n]$, $I_l^{\mathrm{MAI}}[n]$, $I_l^{\mathrm{SI}}[n]$, $N_l[n]$, and $J_l[n]$ are, respectively, given by

$$D_l[n]=\sqrt{\frac{P}{2}}d_1[n]T_s\left(\alpha_l^{(1)}[n]\right)^2 \quad (7)$$

$$\begin{aligned}I_l^{\mathrm{MAI}}[n]=&\sqrt{\frac{P}{2}}\sum_{k=2}^{K_u}\sum_{j=0}^{L-1}\alpha_l^{(1)}[n]\alpha_j^{(k)}[n]\\&\times\Big(d_k[n-1]R_{k,1}\left(\tau_{l,j}^{(k)}[n]\right)+d_k[n]\\&\quad\widehat{R}_{k,1}\left(\tau_{l,j}^{(k)}[n]\right)\Big)\cos\left(\psi_{l,j}^{(k)}[n]\right)\end{aligned} \quad (8)$$

$$\begin{aligned}I_l^{\mathrm{SI}}[n]=&\sqrt{\frac{P}{2}}\sum_{i=0,i=l}^{L-1}\alpha_l^{(1)}[n]\alpha_i^{(1)}[n]\\&\times\Big(d_1[n-1]R_{1,1}\left(\tau_{l,i}^{(1)}[n]\right)+d_1[n]\\&\quad\widehat{R}_{1,1}\left(\tau_{l,i}^{(1)}[n]\right)\Big)\cos\left(\psi_{l,i}^{(1)}[n]\right)\end{aligned} \quad (9)$$

$$N_l[n]=\int_{lT_c}^{lT_c+T_s}n(t)\alpha_l^{(1)}[n]a^{(1)}(t-lT_c)\times\cos\left(w_c t+\psi_l^{(1)}[n]\right)dt \quad (10)$$

$$\text{and}\quad J_l[n]=\int_{lT_c}^{lT_c+T_s}J(t)\alpha_l^{(1)}[n]a^{(1)}(t-lT_c)\times\cos\left(w_c t+\psi_l^{(1)}[n]\right)dt \quad (11)$$

where, for $k=2,\ldots,K_u$, $\tau_{l,j}^{(k)}[n]=\tau_j^{(k)}[n]-\tau_l^{(1)}[n]$, $\psi_{l,j}^{(k)}[n]=\psi_j^{(k)}[n]-\psi_l^{(1)}[n]$, and the partial correlation coefficients $R_{k,1}(\cdot)$ and $\widehat{R}_{k,1}(\cdot)$ are defined as $R_{k,1}(\tau)=\int_0^{\tau}a^{(k)}(t-\tau)a^{(1)}(t)dt$ and $\widehat{R}_{k,1}(\tau)=\int_{\tau}^{T_s}a^{(k)}(t-\tau)a^{(1)}(t)dt$.

We are interested in obtaining the statistics of Z_n at the output of the RAKE receiver. For analytical tractability, conditioned on $\{\alpha_l^{(1)}[n]\}$ and $a^{(1)}(t)$, for a large number of users, we model the interference terms of (8)–(11) as Gaussian processes and obtain the following conditional variance [13], [14]:

$$\left(\sigma_l^{\mathrm{MAI}}[n]\right)^2=\frac{PT_sT_c}{6}\left(\alpha_l^{(1)}[n]\right)^2(K_u-1)\Omega_T \quad (12)$$

with Ω_T is defined as

$$\Omega_T=\sum_{l=0}^{L-1}\Omega_l. \quad (13)$$

For a large number of users, the contribution of self-interference is negligible compared with the MAI, allowing us to ignore the contribution due to $I_l^{\mathrm{SI}}[n]$. The variance of the component due to the AWGN can be computed as [13], [14]

$$\left(\sigma_l^{N}[n]\right)^2=E\left[\left(N_l[n]\right)^2\right]=\frac{T_s\eta_0}{4}\left(\alpha_l^{(1)}[n]\right)^2 \quad (14)$$

whereas the variance of the jammer's contribution, after some algebra, can be shown to be

$$\begin{aligned}\left(\sigma_l^{J}[n]\right)^2&=E\left[\left(J_l[n]\right)^2\right]\\&=\left(\alpha_l^{(1)}[n]\right)^2T_s\frac{1}{4}\\&\quad\times\int_{-\infty}^{\infty}|H(f)|^2\left(S_J(f-f_c)+S_J(f+f_c)\right)\frac{df}{T_c}\\&=\left(\alpha_l^{(1)}[n]\right)^2T_s\frac{\eta_J}{4}\int_{-\frac{W_J}{2}}^{\frac{W_J}{2}}|H(f)|^2\frac{df}{T_c}\end{aligned} \quad (15)$$

where $H(f)$ is the Fourier transform of $h_{T_c}(t)$. Let us define by $\rho_J=W_J/W$ the fraction of the total bandwidth occupied by the jammer, where $W=1/T_c$ is the CDMA system bandwidth. Let $\mathrm{JSR}=\eta_J W_J/P=\mathcal{N}_J/P$ denote the jammer-to-signal power ratio, and $\gamma_b=PT_b/N_0=E_b/N_0$ denote the signal-to-noise ratio (SNR) per information bit. We also define $\zeta_J=\int_{-W_J/2}^{W_J/2}|H(f)|^2df/T_c=\int_{-\rho_J/2}^{\rho_J/2}(\sin^2\pi u/\pi^2u^2)du$. Using integration by parts, ζ_J can be simplified as $\zeta_J=2(\cos(\pi\rho_J)-1)/(\pi^2\rho_J)+(2/\pi)\mathrm{Si}[\pi\rho_J]$, where $\mathrm{Si}[u]=\int_0^u(\sin(t)/t)dt$ [19], so that (15) can be simplified to

$$\left(\sigma_l^{J}[n]\right)^2=\left(\alpha_l^{(1)}[n]\right)^2\frac{\eta_0}{4}\frac{T_s\mathrm{JSR}\gamma_b r_c}{\mathcal{S}_F\rho_J}\zeta_J. \quad (16)$$

Using the results of (12)–(15), the decision statistic Z_n at the output of the RAKE receiver for the nth symbol is given by

$$Z_n = d_1[n]T_s\sqrt{\frac{P}{2}}\sum_{l=0}^{L-1}\left(\alpha_l^{(1)}[n]\right)^2 + \eta_e[n] \tag{17}$$

where $\eta_e[n]$ is approximately Gaussian with zero-mean and variance $\sigma_e^2[n] = \sum_{l=0}^{L-1}(\alpha_l^{(1)}[n])^2 N_e/2$, and

$$N_e \triangleq 2PT_s^2\left\{\frac{(K_u-1)\Omega_T}{6\mathcal{S}_F} + \frac{\eta_0}{4PT_s} + \frac{\eta_0}{4PT_s}\frac{\mathrm{JSR}\gamma_b r_c\zeta_J}{\mathcal{S}_F\rho_J}\right\}. \tag{18}$$

D. Frame Error Rate (FER) With Convolutional Coding

The RAKE receiver outputs, $\{Z_n\}$, corresponding to a given coded frame, are passed to the deinterleaver and are then used by the Viterbi decoder for soft-decision decoding. For convenience, let us define $\beta_n = \sum_{l=0}^{L-1}(\alpha_l^{(1)}[n])^2$, and $\underline{\beta} = (\beta_1,\ldots,\beta_N)$, where N is the frame length, and, for simplicity, we have dropped the index of the desired user. It is well known that at high SNR, the key performance metric with channel coding is the pairwise error probability between two codewords [15]. The PEP between two codewords $\mathbf{x} = (x_1,\ldots,x_N)$ and $\mathbf{y} = (y_1,\ldots,y_N)$ which differ in d positions is given by

$$\begin{aligned}P_2(d|\underline{\alpha}) &= \mathrm{Prob}\left(\sum_{n=1}^{N}(z_n-x_n)^2 > \sum_{n=1}^{N}(z_n-y_n)^2\right)\\ &= \mathrm{Prob}\left(\sum_{n=1}^{N} z_n(x_n-y_n) < 0\right)\\ &= \mathrm{Prob}\left(\sum_{n=1}^{N}\eta_e[n](x_n-y_n) < -\sqrt{\frac{PT_s^2}{2}}\right.\\ &\qquad \left.\times\sum_{n=1}^{N}\beta_n x_n(x_n-y_n)\right)\end{aligned} \tag{19}$$

where in the last step of (19) we have used (17). Without loss of generality, we assume that the codewords $\mathbf{x}$ and $\mathbf{y}$ differ in the first d positions. Then, using the Chernoff bound, $Q(x) \le 1/2\exp(-x^2/2)$ for $x \ge 0$, we can upper bound (19) as

$$P_2(d|\underline{\beta}) \le \frac{1}{2}\exp\left(-\Gamma\sum_{n=1}^{d}\beta_n\right) \tag{20}$$

where Γ is the signal-to-interference-plus-noise ratio and is given by

$$\Gamma = \frac{\frac{PT_s}{N_0}}{1+\frac{PT_s}{N_0\mathcal{S}_F}\left\{\frac{2}{3}(K_u-1)\Omega_T + \frac{\mathrm{JSR}\zeta_J}{\rho_J}\right\}} = \frac{r_c\gamma_b}{1+\frac{r_c\gamma_b}{\mathcal{S}_F}\Delta} \tag{21}$$

and where we have used $T_s = r_cT_b$, $E_b = PT_b$, and $\Delta = 2/3(K_u-1)\Omega_T + (\mathrm{JSR}\zeta_J/\rho_J)$. Note that Δ, being a function of the multipath channel profile, the number of active users, and the JSR, is independent of r_c, $\mathcal{S}_F$, and the SNR-per-bit of the desired user, γ_b. Upon taking the expectation of (20) over the distribution of (3), we obtain

$$\begin{aligned}\overline{P}_2(d) = E\left\{P_2(d|\underline{\beta})\right\} &\le \frac{1}{2}\prod_{l=0}^{L-1}\left(\frac{m_l}{m_l+\Gamma\Omega_l}\right)^{m_l d}\\ &< \frac{1}{2}\prod_{l=0}^{L-1}\left(\frac{m_l}{\Omega_l}\right)^{m_l d}\Gamma^{-d\sum_{l=0}^{L-1}m_l}\\ &= C(\underline{m},\underline{\Omega},d)\Gamma^{-md}\end{aligned} \tag{22}$$

where $m = \sum_{l=0}^{L-1}m_l$, $\underline{m} = (m_0,\ldots,m_{L-1})$, $\underline{\Omega} = (\Omega_0,\ldots,\Omega_{L-1})$, and $C(\underline{m},\underline{\Omega},d) = (1/2)\prod_{l=0}^{L-1}(m_l/\Omega_l)^{m_l d}$. In this paper, we assume that the maximum average signal-to-interference-plus-noise ratio, $\overline{\Gamma}_{\max} = \Gamma\times\max(\Omega_l)$ is at least greater than unity (i.e., above 0 dB).

An exact expression for the frame error rate (FER) for a convolutional code with soft-decision decoding is difficult to derive, which motivates us to employ the union bound, as it is sufficiently tight at high SNRs. A tight upper bound on the FER of a convolutional code with block lengths larger than the constraint length is obtained in [9], using which we obtain the FER for our system as

$$P_B \le \sum_d t(d)\overline{P}_2(d) < \sum_d t(d)C(\underline{m},\underline{\Omega},d)\Gamma^{-md} \tag{23}$$

where $t(d)$ is a function of the weight spectrum [15] of the underlying convolutional code. We are also interested in a lower bound on the FER, which can be obtained by taking only the dominant term of (23). However, the Chernoff upper bound on PEP of (22) is no longer useful. In Appendix A, we derive a lower bound for $\overline{P}_2(d)$, using which the lower bound on the FER can be obtained as

$$P_B \ge t(d_{\mathrm{free}})D(m,d_{\mathrm{free}})(1+\Gamma\omega)^{-md_{\mathrm{free}}} \tag{24}$$

where d_{free} is the free distance of the code, and $D(m,d)$ and ω are defined in Appendix A.

III. End-to-End Average Distortion

We assume that the information source is Gaussian-distributed with independent and identically distributed (i.i.d.) source samples, each with unit variance. If r_s denotes the number of bits-per-source sample, then the average source distortion with minimum mean square error scalar quantization on a noise-free channel is approximated, for large r_s, as $D(r_s) = \epsilon 2^{-2r_s}$, where ϵ depends on the quantizer [16]. Note that each coded frame of length N contains Nr_c/r_s source samples. Then, the average distortion per source sample can be written as [17, eq. (10)]

$$\begin{aligned}&\mathcal{D}(r_s,r_c,\mathcal{S}_F)\\ &\quad= \frac{\frac{Nr_c}{r_s}\left(1-P_B(r_c,\mathcal{S}_F)\right)\epsilon 2^{-2r_s} + \frac{Nr_c}{r_s}P_B(r_c,\mathcal{S}_F)}{\frac{Nr_c}{r_s}}\\ &\quad= \left(\left(1-P_B(r_c,\mathcal{S}_F)\right)\epsilon 2^{-2r_s} + P_B(r_c,\mathcal{S}_F)\right)\\ &\quad\le \left(\epsilon 2^{-2r_s} + P_B(r_c,\mathcal{S}_F)\right)\\ &\quad\le \left(\epsilon 2^{-2r_s} + \sum_d t(d)C(\underline{m},\underline{\Omega},d)\Gamma^{-md}\right)\\ &\quad\triangleq D_u(r_s,r_c,\mathcal{S}_F)\end{aligned} \tag{25}$$

where the above upper bound is quite accurate in the high SNR region. Note that the term $t(d)$ of (25) depends on the number of input and output bits, and on the particular encoder used to realize the convolutional code of a given rate. It also depends on the code's constraint length[1] (i.e., the number of memory elements used). Unfortunately, in general, a functional relationship between $t(d)$ and r_c is not known.

A lower bound on the end-to-end average distortion can be obtained by first lower bounding the FER, $P_B(r_c, \mathcal{S}_F)$ by the term with minimum free distance d_{free} as $P_B(r_c, \mathcal{S}_F) \geq t(d_{\text{free}})P_2(d_{\text{free}})$. With this, a lower bound on the average distortion can be obtained as

$$\begin{aligned} D(r_s, r_c, \mathcal{S}_F) &\geq \epsilon 2^{-2r_s} + t(d_{\text{free}})P_2(d_{\text{free}})(1-\epsilon 2^{-2r_s}) \\ &= \epsilon 2^{-2r_s} + t(d_{\text{free}})D(m, d_{\text{free}}) \\ &\quad \times (1+\Gamma\omega)^{-md_{\text{free}}}(1-\epsilon 2^{-2r_s}) \\ &\triangleq D_{\text{lower}}(r_s, r_c, \mathcal{S}_F) \end{aligned} \tag{26}$$

where, in the second step of (26), we have used (24).

In what follows, we consider both the upper bound and lower bound on the average distortion (25) and (26) as our objective functions.

IV. Optimum Bandwidth Allocation

If we denote by $\mathcal{U}$ the number of source samples per second available to the source coder, then the total rate at the output of the spread-spectrum modulator is given by $\mathcal{U}r_s(1/r_c)\mathcal{S}_F$, which should not exceed the spread-spectrum bandwidth W. That is, the variables r_s, r_c, and $\mathcal{S}_F$ are related by $r_s\mathcal{S}_F/r_c \leq C_0$, where $C_0 = W/\mathcal{U}$. The distortion function is given by $D(r_s, r_c, \mathcal{S}_F)$, which can also be written as $D(r_s, r_c, C_0 r_c/r_s)$. We notice that by fixing the channel code rate r_c the distortion can be expressed only as a function of the source rate r_s together with the bandwidth constraint C_0. In this section, we minimize the objective functions, $D_u(r_s, r_c, \mathcal{S}_F)$ of (25) and $D_{\text{lower}}(r_s, r_c, \mathcal{S}_F)$ of (26), as a function of the source code rate r_s.

A. Optimal Allocation Based on Upper Bound

With r_c fixed, we substitute $\mathcal{S}_F = C_0 r_c/r_s$ in Γ of (25) and simplify (25) in the form of a function of r_s alone as

$$D_u(r_s) = \epsilon 2^{-2r_s} + \sum_d t(d)C(\underline{m}, \underline{\Omega}, d)(r_c\gamma_b)^{-md} \times \left(1 + \frac{\gamma_b\Delta}{C_0} r_s\right)^{md}. \tag{27}$$

[1]Even for the same code rate, and the same constraint length, different generator polynomials result in different weight spectra $t(d)$ [15].

Differentiating (27) with respect to r_s we arrive at

$$\frac{d}{dr_s}D_u(r_s) = -\epsilon 2\ln 2 2^{-2r_s} + \sum_d t(d)C(\underline{m}, \underline{\Omega}, d)(r_c\gamma_b)^{-md} \times md\frac{\gamma_b\Delta}{C_0}\left(1 + \frac{\gamma_b\Delta}{C_0} r_s\right)^{md-1}. \tag{28}$$

If r_s^* is the optimum source code rate, then we have $(d/dr_s)D_u(r_s)|_{r_s=r_s^*} = 0$. Equivalently, r_s^* satisfies (29) shown at the bottom of the page. The second derivative of $D_u(r_s)$ can be calculated by differentiating (28) with respect to r_s and results in

$$\frac{d^2}{dr_s^2}D_u(r_s) = 4\epsilon(\ln 2)^2 2^{-2r_s} + \sum_d t(d)C(\underline{m}, \underline{\Omega}, d)(r_c\gamma_b)^{-md} \times md(md-1)\left(1 + \frac{\gamma_b\Delta}{C_0} r_s\right)^{md-2}\left(\frac{\gamma_b\Delta}{C_0}\right)^2. \tag{30}$$

Equation (30) is always positive, since $m = \sum_{l=0}^{L-1} m_l \geq L/2$ and $md \geq Ld/2 > 1$, showing that $D_u(r_s)$ is a convex function of r_s. The optimal three-tuple is then given by $(r_s^*, r_c, C_0 r_c/r_s^*)$, where r_s^* can be obtained by solving (29).

B. Optimal Allocation Based on Lower Bound

Upon taking the first derivative of (26) with respect to r_s, we obtain

$$\begin{aligned} &\frac{d}{dr_s}D_{\text{lower}}(r_s) \\ &\quad = -\epsilon(2\ln 2)2^{-2r_s} + t(d_{\text{free}})D(m, d_{\text{free}}) \\ &\qquad \times (1+\Gamma\omega)^{-md_{\text{free}}}\epsilon(2\ln 2)2^{-2r_s} + t(d_{\text{free}}) \\ &\qquad \times D(m, d_{\text{free}})(1-\epsilon 2^{-2r_s}) \\ &\qquad \times \left(-md_{\text{free}}\omega(1+\Gamma\omega)^{-md_{\text{free}}-1}\frac{d\Gamma}{dr_s}\right) \end{aligned} \tag{31}$$

where

$$\frac{d\Gamma}{dr_s} = -\frac{r_c\gamma_b\frac{\gamma_b\Delta}{C_0}}{\left(1 + r_s\frac{\gamma_b\Delta}{C_0}\right)^2} = -\Gamma\frac{\frac{\gamma_b\Delta}{C_0}}{1 + r_s\frac{\gamma_b\Delta}{C_0}} \tag{32}$$

which is $< 0 \forall r_s$. In Appendix B, we prove that $D_{\text{lower}}(r_s)$ is a convex function of r_s. Upon setting $d/dr_s D_{\text{lower}}(r_s) = 0$ and solving for r_s, we arrive at the following implicit equation (33) shown at the bottom of the next page, where $\Gamma^* = \Gamma$ evaluated at $r_s = r_s^*$.

V. Results and Discussion

In this section, we present some numerical results based on the analysis presented in Sections II–IV. Unless otherwise stated, it is assumed that the energy-per-bit (equivalently,

$$r_s^* = \frac{1}{2}\log_2\left(\frac{2\epsilon\ln 2}{\sum_d t(d)C(\underline{m}, \underline{\Omega}, d)(r_c\gamma_b)^{-md} md\frac{\gamma_b\Delta}{C_0}\left(1 + \frac{\gamma_b\Delta}{C_0} r_s^*\right)^{md-1}}\right) \tag{29}$$

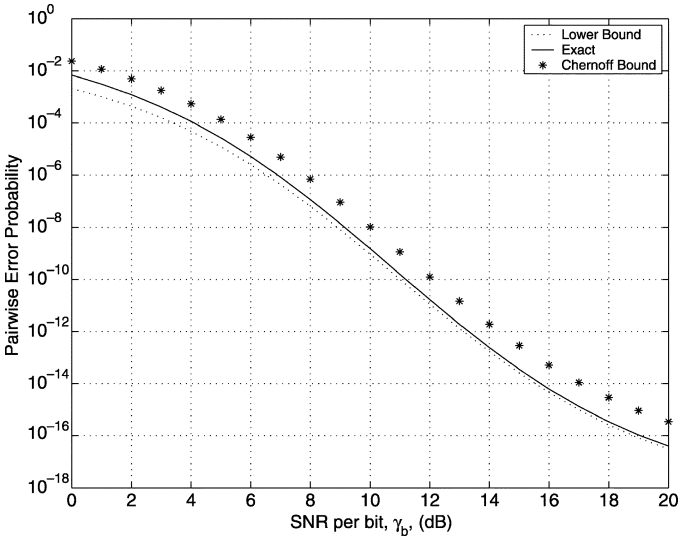

Fig. 2. Comparison of exact pairwise error probability with the one based on the Chernoff bound and the one based on a lower bound. Distance between two code words is set to ten. The system parameters are the following: $K_u = 25$, $\mathrm{JSR} = 5$ dB, $\rho_J = 0.2$, $r_c = 1/3$, $\mathcal{S}_F = 128$, and $L = 4$. We assume i.i.d. Rayleigh fading. That is, $\underline{m} = (1, 1, 1, 1)$ and $\underline{\Omega} = (1, 1, 1, 1)$.

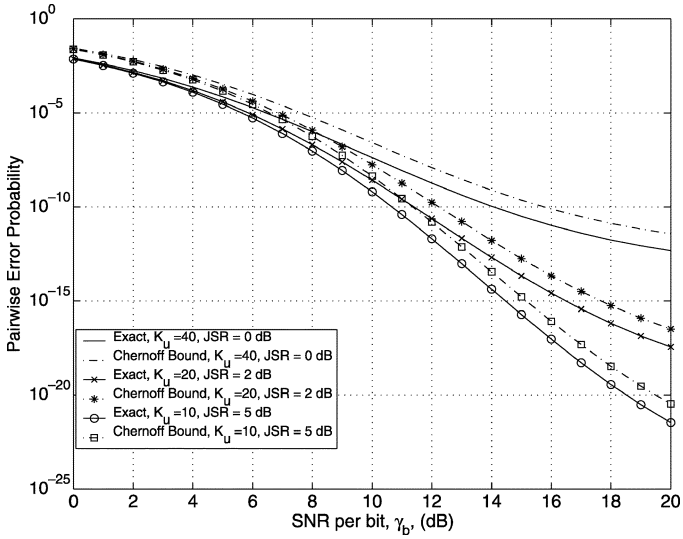

Fig. 3. Comparison of exact pairwise error probability with the one based on the Chernoff bound. Distance between two code words is set to ten. $\rho_J = 0.2$, channel code rate $r_c = 1/3$, and spreading factor $\mathcal{S}_F = 128$. Number of multipaths, $L = 4$ with $\underline{m} = (0.5, 1, 2.5, 5)$ and $\Omega_l = \exp(-\delta(l-1))$, $l = 1, \ldots, L$, where δ is the decay parameter for the multipath intensity profile which is set to 0.5.

the SNR-per-bit, γ_b) is kept constant. First, Fig. 2 shows the tightness of the lower and the upper bounds on the PEP for a frequency-selective i.i.d. Rayleigh-fading channel with $L = 4$ paths. Also shown is the true PEP from (35) in Appendix A, which is numerically evaluated. We conclude from Fig. 2 that the bounds are sufficiently tight. In particular, for SNR-per-bit, γ_b, values less than 15 dB, the upper bound is within 2 dB of the true PEP. Fig. 3 shows the effect of varying both JSR and K_u on the upper bound on the PEP for an exponentially decaying Nakagami multipath channel with $L = 4$ paths. From Fig. 3, we note that for smaller values of JSR and K_u, the bound is within 2 dB of the true PEP for γ_b less than or equal to 20 dB.

The lower and upper bounds on the average end-to-end source distortion, as derived in Section III, are plotted in Fig. 4. For a fixed spread bandwidth and channel code rate, the average distortion is plotted as a function of the source code rate. A family of such curves is obtained for varying levels of channel code complexity, as measured by its constraint length. We notice from Fig. 4 that: 1) there exists a source code rate at which the distortion is minimized; 2) the minimum source code rate shifts to the right for increasing values of the channel code complexity, since a stronger channel code enables the spread-spectrum modulator to use a smaller value of the spread factor; 3) the lower and the upper bounds coincide at values of r_s that are near the r_s at which the distortion is minimized, after which the bounds differ by an order of magnitude. This difference in the lower and the upper bounds can be explained as follows: For small values of r_s (i.e., large $\mathcal{S}_F$), the upper and lower bounds on the FER are tight, resulting in a tight bound on the end-to-end distortion.

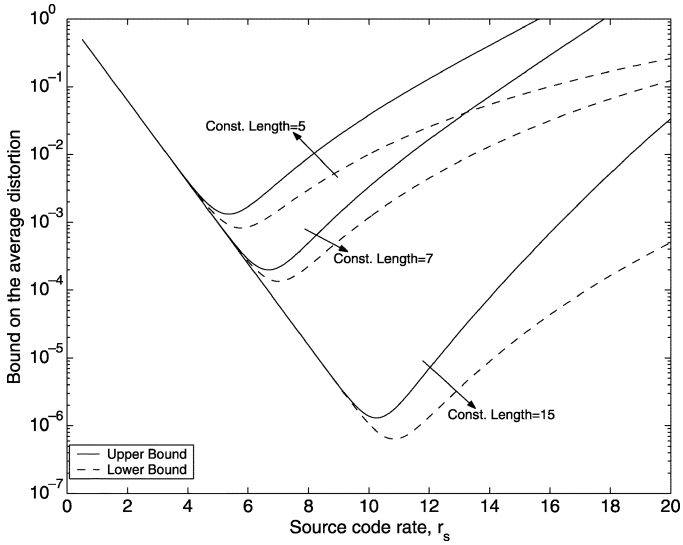

Fig. 4. Lower and upper bounds on the average distortion on i.i.d. Rayleigh-fading channels with $L = 4$ multipath components. The channel code rate is fixed to $r_c = 1/2$ and the bandwidth expansion factor is set to 500. Binary convolutional codes with various constraint lengths are used with an optimum distance spectrum, as given in [10]. The other system parameters are: $\mathrm{JSR} = 5$ dB, $\rho_J = 0.25$, $K_u = 15$, and $\gamma_b = 10$ dB.

$$r_s^* = \frac{1}{2}\log_2\left\{\epsilon + \frac{\epsilon 2\ln 2\left(1 - t(d_{\text{free}})D(m, d_{\text{free}})(1+\Gamma^*\omega)^{-md_{\text{free}}}\right)}{t(d_{\text{free}})D(m, d_{\text{free}})(1+\Gamma^*\omega)^{-md_{\text{free}}-1}md_{\text{free}}\omega\left(-\left.\frac{d\Gamma}{dr_s}\right|_{r_s=r_s^*}\right)}\right\} \tag{33}$$

TABLE I
SOURCE CODE RATE, SPREADING FACTOR, AND THE MINIMUM DISTORTION, FOR A FIXED CHANNEL CODE RATE BASED ON BOTH UPPER AND LOWER BOUNDS ON THE END-TO-END AVERAGE DISTORTION. BOTH I.I.D. AND NON-I.I.D. RAYLEIGH-FADING CHANNELS ARE CONSIDERED, WITH A MULTIPATH INTENSITY PROFILE (MIP) PARAMETER $\delta = 0.5$ FOR THE CASE OF NON-I.I.D. FADING

r_c	Channel	Lower Bound			Upper Bound		
		r_s^*	$\mathcal{S}_F = C_0 r_c / r_s^*$	$D(r_s^*)$	r_s^*	$\mathcal{S}_F = C_0 r_c / r_s^*$	$D(r_s^*)$
$\frac{1}{2}$	i.i.d	6.33	39	$3.04 \cdot 10^{-4}$	5.68	43	$6.56 \cdot 10^{-4}$
	non-i.i.d	8.81	28	1.02×10^{-5}	5.50	45	$8.44 \cdot 10^{-4}$
$\frac{1}{3}$	i.i.d	7.01	23	$1.17 \cdot 10^{-4}$	6.30	26	$2.74 \cdot 10^{-4}$
	non-i.i.d	9.78	17	$2.63 \cdot 10^{-6}$	6.17	27	$3.33 \cdot 10^{-4}$
$\frac{1}{4}$	i.i.d	6.95	17	$1.20 \cdot 10^{-4}$	6.53	19	$2.01 \cdot 10^{-4}$
	non-i.i.d	9.86	12	$2.23 \cdot 10^{-6}$	6.42	19	$2.35 \cdot 10^{-4}$

This explains the behavior of the curves to the left of the minimum. However, when r_s increases, we have a smaller value for $\mathcal{S}_F$, and the Chernoff-based union bound is found to be less effective, and not comparable with the dominant term-based lower bound. This results in a large difference between the upper and lower bounds.

In Table I, we present the optimum source code rate, the optimum spreading factor, and the resulting average distortion for various channel code rates. For all the channel codes, the complexity of the encoder is fixed at a constraint length of 6. Both lower and upper bounds on the distortion are considered for both i.i.d. and non-i.i.d. Rayleigh channels, with the constraint on the bandwidth expansion factor set to 500 (i.e., $r_s(1/r_c)\mathcal{S}_F = 500$). The number of users is fixed at $K_u = 15$. From Table I, we observe that for both i.i.d. and non-i.i.d. fading conditions, the lower bound favors allocating more bandwidth to the source coder, whereas the upper bound favors increasing the spread factor. This is due to the fact that the lower bound-based end-to-end distortion is much smaller in comparison with the union upper bound-based one, and by increasing the spread factor (i.e., by reducing r_s) the upper bound-based distortion can be minimized. Table I also indicates that with decreasing channel code rates, it is beneficial to allocate more bandwidth to the source coder rather than to the spread-spectrum modulator. This can be explained as follows: For a given constraint length, a low rate channel code provides higher free distance and, hence, a larger diversity order, which helps to reduce the burden on the spread-spectrum modulator.

By fixing the channel code rate at $r_c = 1/2$, and for constraint lengths of 7 and 15, r_s and $D_u(r_s)$ are plotted as a function of the bandwidth expansion factor in Figs. 5 and 6, respectively. Both Rayleigh- (i.e., $m = 1$) and Nakagami-fading channels are considered, with the Nakagami parameter of the latter channel set to five. From Fig. 5, we notice that as the total bandwidth increases, the source code rate increases. It is also evident that this allocation increases with the constraint length of the channel code, and with the fading severity index m of the Nakagami channel. That is, lighter fading (i.e., increasing m) and/or powerful channel coding result in higher source code rate. Although not shown in Fig. 5, we have also found that, while the spreading factor also increases with the total bandwidth, it does not increase as rapidly as the source code rate. Fig. 6 shows the resulting minimum distortion based on the optimum source code rates obtained in Fig. 5. The average distortion decreases with

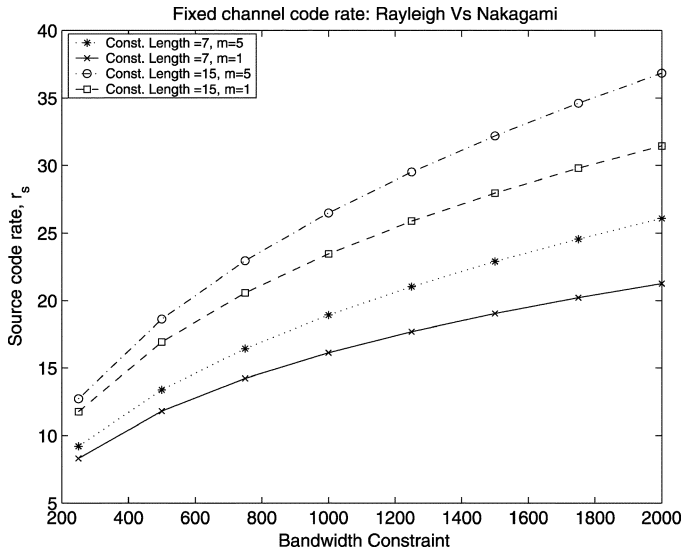

Fig. 5. Source code rate, for a fixed channel code, obtained using the upper bounds on the average distortion on i.i.d. fading channels with $L = 4$ multipath components. Both Rayleigh fading and Nakagami fading with $m = 5$ are assumed. The channel code rate is fixed to $r_c = 1/2$ and the bandwidth expansion factor is varied. Number of information bits in the frame is set to 100. The other system parameters are: $\gamma_b = 10$ dB, $K_u = 10$, JSR $= 5$ dB, and $\rho_J = 0.25$.

the bandwidth expansion factor, the Nakagami parameter m, and the constraint length of the channel code.

In [9], some of the numerical results were obtained by fixing $E_c/N_0 = PT_c/N_0$ (i.e., the SNR per chip) instead of the SNR per bit $\gamma_b = (PT_c/N_0)\mathcal{S}_F/r_c$. Fig. 7 shows the tradeoff curves parameterized by E_c/N_0. Note that for a fixed E_c/N_0, the spread factor increases with the bandwidth expansion factor. This can be explained as follows: For a fixed E_c/N_0, increasing the spread factor has two effects on the system performance: 1) a larger $\mathcal{S}_F$ reduces the interference from the other users and 2) a larger $\mathcal{S}_F$ leads to an increase in the SNR per bit, since $\gamma_b = \mathcal{S}_F(E_c/(N_0 r_c))$. However, the channel gets better with increasing E_c/N_0, and we do not need as large a γ_b, so we can reduce $\mathcal{S}_F$, and allocate more bandwidth to the source.

The effect of increasing the jammer's bandwidth on the tradeoff performance is now discussed. The source code rate and the resulting distortion are shown in Figs. 8 and 9, respectively. The fraction of the jammer's bandwidth $\rho_J = W_J/W$ is chosen from $\{0.1, 0.5, 0.9\}$. The JSR is set to 10 dB, $\gamma_b = 15$ dB,

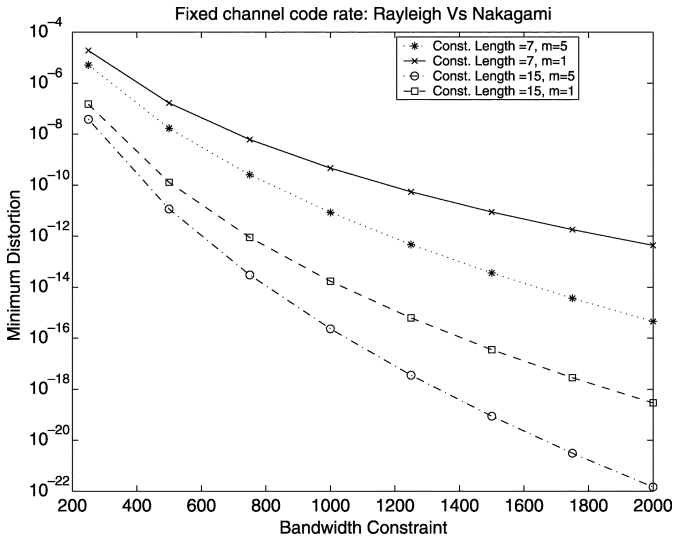

Fig. 6. Average distortion obtained using the source code rate of Fig. 5, for a fixed channel code on i.i.d. fading channels with $L = 4$ multipath components. Both Rayleigh fading and Nakagami fading with $m = 5$ are assumed. The channel code rate is fixed to $r_c = 1/2$ and the bandwidth expansion factor is varied. Number of information bits in the frame is set to 100. The other system parameters are: $\gamma_b = 10$ dB, $K_u = 10$, $\mathrm{JSR} = 5$ dB, and $\rho_J = 0.25$.

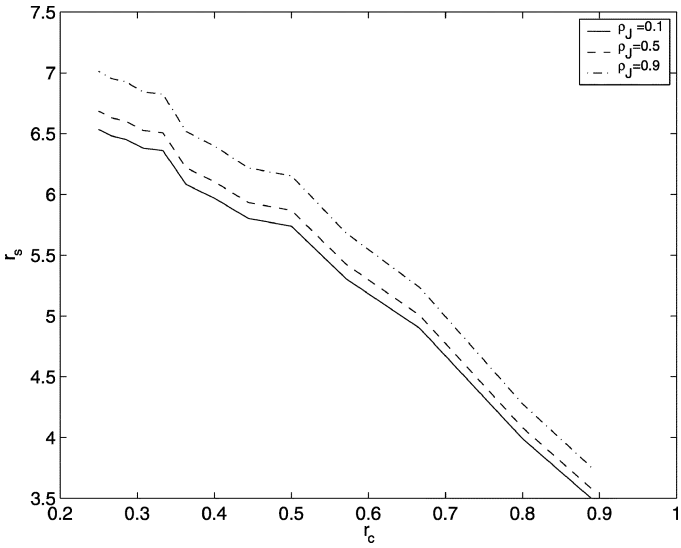

Fig. 8. Source code rate as a function of the channel code rate, parameterized by the fraction of the jammer's bandwidth $\rho_J = W_J/W$. An RCPC code, with a mother code rate of 1/4, is used with a frame length of 500 information bits. The other system parameters are: $\gamma_b = 15$ dB, $K_u = 10$, $\mathrm{JSR} = 10$ dB, and $C_0 = 500$. Rayleigh-fading channel with $L = 4$ paths with uniform multipath intensity profile is assumed.

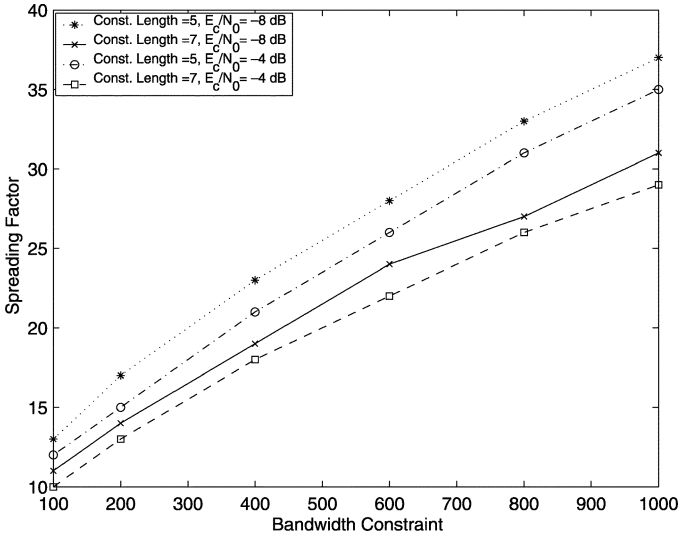

Fig. 7. Spreading factor $\mathcal{S}_F$ for a fixed channel code, obtained using the upper bounds on the average distortion on i.i.d. Rayleigh-fading channels with $L = 4$ multipath components. The channel code rate is fixed to $r_c = 1/2$ and the bandwidth expansion factor is varied. Number of information bits in the frame is set to 100. The other system parameters are: $E_c/N_0 = PT_c/N_0$, $K_u = 10$, $\mathrm{JSR} = 5$ dB, and $\rho_J = 0.25$.

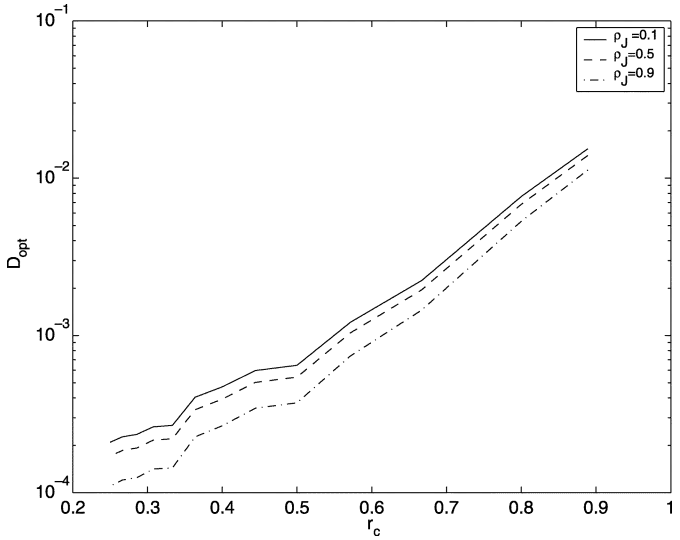

Fig. 9. Minimum source distortion as a function of the channel code rate, parameterized by the fraction of the jammer's bandwidth $\rho_J = W_J/W$. An RCPC code, with a mother code rate of 1/4, is used with a frame length of 500 information bits. The other system parameters are: $\gamma_b = 15$ dB, $K_u = 10$, $\mathrm{JSR} = 10$ dB, and $C_0 = 500$. Rayleigh-fading channel with $L = 4$ paths with uniform multipath intensity profile is assumed.

and $K_u = 10$. We have used rate-compatible punctured convolutional (RCPC) codes with a base code rate of 1/4 [20] and a frame length of 500 bits. The channel exhibits Rayleigh fading with a uniform MIP with $L = 4$ paths. Note that, from Fig. 8, when r_s is fixed, the tradeoff problem is reduced to that of a channel coding-spreading tradeoff problem. In this scenario, the expression $\Gamma = r_c\gamma_b/(1+r_c\gamma_b\Delta/\mathcal{S}_F) = r_c\gamma_b/(1+r_s\gamma_b\Delta/C_0)$ of (21) increases with both increasing r_c and increasing ρ_J. Hence, for a fixed r_s, the channel code rate increases with increasing ρ_J and, thus, the spreading factor increases. However, as seen in Fig. 8, when r_c is fixed, the source code rate increases with increasing ρ_J and, thus, the spreading factor decreases. Finally, Fig. 9 shows that the average distortion decreases with increasing ρ_J.

We also investigated the effect of increasing system load (i.e., the number of users K_u) on the bandwidth allocation. The results are summarized in Table II, which correspond to constant MIP Rayleigh-fading channels with $L = 4$ paths, $\gamma_b = 20$ dB, and $\mathrm{JSR} = 0$ dB. The bandwidth constraint is set to 500. From Table II, for a given channel code rate, it is seen that the source code rate has to be decreased as the number of users increases to allow sufficient processing gain to suppress the additional MAI.

TABLE II
SOURCE CODE RATE, SPREADING FACTOR, AND THE MINIMUM DISTORTION, FOR A FIXED CHANNEL CODE RATE, BASED ON BOTH UPPER AND LOWER BOUNDS ON THE END-TO-END AVERAGE DISTORTION. AN I.I.D. RAYLEIGH-FADING CHANNEL IS ASSUMED WITH $L = 4$ PATHS. THE OTHER SYSTEM PARAMETERS ARE AS FOLLOWS: SNR-PER-BIT, $\gamma_b = 20$ dB, JSR $= 0$ dB, AND $\rho_J = 0.25$. THE BANDWIDTH CONSTRAINT C_0 IS SET TO 500. THE CONSTRAINT LENGTH OF THE CHANNEL CODE IS FIXED TO 6

r_c	K_u	Lower Bound			Upper Bound		
		r_s^*	$\mathcal{S}_F = C_0 r_c / r_s^*$	$D(r_s^*)$	r_s^*	$\mathcal{S}_F = C_0 r_c / r_s^*$	$D(r_s^*)$
$\frac{1}{2}$	10	11.78	21	$1.715 \cdot 10^{-7}$	11.40	21	$2.742 \cdot 10^{-7}$
	25	7.30	34	$7.683 \cdot 10^{-5}$	6.74	37	$1.495 \cdot 10^{-4}$
	50	4.95	50	$1.863 \cdot 10^{-3}$	4.29	58	$3.954 \cdot 10^{-3}$
$\frac{1}{3}$	10	13.12	12	$2.582 \cdot 10^{-8}$	12.68	13	$4.516 \cdot 10^{-8}$
	25	8.06	20	$2.671 \cdot 10^{-5}$	7.44	22	$5.651 \cdot 10^{-5}$
	50	5.45	30	$9.236 \cdot 10^{-4}$	4.74	35	$2.124 \cdot 10^{-3}$
$\frac{1}{4}$	10	13.41	9	$1.653 \cdot 10^{-8}$	13.13	9	$2.353 \cdot 10^{-8}$
	25	8.05	15	$2.557 \cdot 10^{-5}$	7.68	16	$4.014 \cdot 10^{-5}$
	50	5.84	21	$6.791 \cdot 10^{-4}$	4.91	25	$1.696 \cdot 10^{-3}$

Also, for a given number of users, the best performance is seen to be achieved at the lowest channel code rate.

Finally, we found the optimal two-tuple (i.e., optimal r_s or $\mathcal{S}_F$) and the resulting minimum average distortion when RCPC codes are used. We used an RCPC code with memory four and a puncturing period of eight, as given in [20]. The code can produce 13 punctured code rates according to a puncturing pattern. Since every possible punctured channel code rate is considered in the optimization, the two-way optimization of r_s and $\mathcal{S}_F$ is equivalent to the joint three-way optimization of r_s, r_c, and $\mathcal{S}_F$. The minimum distortion and the resulting optimum r_s^* and $\mathcal{S}_F^*$ obtained by employing the upper bound are tabulated in Table III as a function of a selected subset of the available rates of the chosen RCPC code.

To carry out the simulation, we could not use the exact optimum values r_s^* and $\mathcal{S}_F^*$ obtained from the analysis. In simulation, the r_s must be restricted to be integers, and the spreading sequence we restricted to be from the set of Gold codes with $\mathcal{S}_F \in \{7, 15, 31, 63\}$. For each value of r_c in Table III, an $(r_s, \mathcal{S}_F)$ pair for simulating the end-to-end distortion was chosen to approximately match the optimum $(r_s^*, \mathcal{S}_F^*)$ pair obtained from the upper bound-based analytical results. The pair was chosen by first selecting the $\mathcal{S}_F \in \{7, 15, 31, 63\}$ which is closest to the optimum $\mathcal{S}_F^*$, and then obtaining $r_s = \lfloor C_0 r_c / \mathcal{S}_F \rfloor$. Note that, as illustrated below, picking the $(r_s, \mathcal{S}_F)$ pair that best approximates the corresponding analytically derived pair does not necessarily minimize distortion, because of the differences in accounting for the self-interference.

From Table III, the upper bound-based optimization shows that the minimum distortion decreases with decreasing channel code rate, indicating that the optimal system has no spreading at all. However, the simulated system in Table III shows that decreasing the channel code rate below $r_c = 4/9$ leads to an increase in the distortion. This is due to the fact that, at smaller values of $\mathcal{S}_F$ with $K_u = 12$ users, the system is affected by the self-interference of the user-of-interest, which is neglected in the upper bound-based analysis. To confirm this, we also simulated the system with $r_c = 2/7$ and other pairs of $(r_s, \mathcal{S}_F)$. With $(r_s, \mathcal{S}_F) = (2, 63)$ a distortion value of $6.197 \cdot 10^{-5}$ is observed, and with $(r_s, \mathcal{S}_F) = (4, 31)$ the distortion increases to $5.813 \cdot 10^{-4}$, but both of these are lower than the distortion of $2.714 \cdot 10^{-2}$ reported in Table III with $(r_s, \mathcal{S}_F) = (9, 15)$. For high values of r_c and $\mathcal{S}_F$, the simulated and analytical results are close. However, the simulation shows that for small values of spreading factor, the system indeed suffers from the self-interference of the user-of-interest. The analysis, with its neglect of the self-interference term, underestimates the importance of spreading.

TABLE III
SPREADING FACTOR, AND THE MINIMUM DISTORTION, FOR VARIOUS PUNCTURED CHANNEL CODE RATES FROM A GIVEN RCPC CODE, BASED ON BOTH THE UPPER BOUND AND THE SIMULATIONS ON THE END-TO-END AVERAGE DISTORTION. AN I.I.D. RAYLEIGH-FADING CHANNEL IS ASSUMED WITH $L = 4$ PATHS. THE OTHER SYSTEM PARAMETERS ARE AS FOLLOWS: SNR-PER-BIT, $\gamma_b = 20$ dB, JSR $= 0$ dB, $\rho_J = 0.25$, AND $K_u = 12$. THE BANDWIDTH CONSTRAINT C_0 IS SET TO 500. FOR SIMULATIONS, WE HAVE USED GOLD CODES

	Upper Bound			Simulation		
r_c	Distortion	r_s^*	$\mathcal{S}_F^* = C_0 r_c / r_s^*$	Distortion	r_s	$\mathcal{S}_F$
4/5	$4.491 \cdot 10^{-4}$	6.1538	65	$1.047 \cdot 10^{-4}$	6	63
4/7	$3.185 \cdot 10^{-5}$	8.6580	33	$1.893 \cdot 10^{-5}$	9	31
4/9	$1.068 \cdot 10^{-5}$	8.8889	25	$6.872 \cdot 10^{-6}$	7	31
4/11	$5.968 \cdot 10^{-6}$	9.5694	19	$1.629 \cdot 10^{-5}$	12	15
1/3	$2.926 \cdot 10^{-6}$	9.8039	17	$4.987 \cdot 10^{-3}$	11	15
2/7	$2.353 \cdot 10^{-6}$	10.204	14	$2.714 \cdot 10^{-2}$	9	15

VI. CONCLUSION

For a fixed total bandwidth expansion factor, we have studied the problem of optimal bandwidth allocation among the source coder, the channel coder, and the spread-spectrum unit for a DS-CDMA system operating over a frequency-selective Nakagami-fading channel with Gaussian PBI. Assuming a Gaussian source with the optimum scalar quantizer, and a binary convolutional code with soft-decision decoding, we obtained both a lower and an upper bound on the end-to-end average source distortion. The joint three-way constrained optimization of the source code rate, the channel code rate, and the spreading factor was simplified to an unconstrained optimization problem over two variables. With a fixed channel code rate, it was shown that both upper and lower bound-based distortion functions are convex functions of the source code

rate. However, an explicit solution for the optimum source code rate, that minimizes the average distortion, was difficult to obtain. Numerical results were presented for the optimum source code rate and spreading factor, parameterized by the channel code rate, code constraint length, and various system loads. The optimal bandwidth allocation, in general, depends on the system and the channel conditions, such as the total number of active users, the average JSR power ratio, and the number of resolved multipath components together with their power delay profile.

Appendix A
Lower Bound on the Pairwise Error Probability

We start with the conditional PEP of (19). With the assumption of $\mathbf{x}$ and $\mathbf{y}$ differing in the first d positions, using (21), the conditional PEP of (19) can be conveniently written as

$$P_2(d|\underline{\beta}) = Q\left(\sqrt{2\Gamma\sum_{n=1}^{d}\beta_n^2}\right) = \frac{1}{\pi}\int_{\theta=0}^{\frac{\pi}{2}} d\theta \exp\left(-\frac{\Gamma\sum_{l=0}^{L-1}\sum_{n=1}^{d}\alpha_l^2[n]}{\sin^2\theta}\right) \quad (34)$$

where $Q(x) = 1/\sqrt{2\pi}\int_x^\infty \exp(-u^2/2)du$ and the second step of (34) is due to the alternate representation of as $Q(x) = 1/\pi\int_0^{\pi/2}\exp(-x^2/(2\sin^2\theta))d\theta$, as presented in [18]. Upon averaging (34) over the pdf of $\{\alpha\}$, as given in (3), we obtain

$$\overline{P}_2(d) = \frac{1}{\pi}\int_{\theta=0}^{\frac{\pi}{2}} d\theta \prod_{l=0}^{L-1}\left(\frac{\sin^2\theta}{\sin^2\theta+\frac{\Gamma\Omega_l}{m_l}}\right)^{m_l d}. \quad (35)$$

A lower bound on $\overline{P}_2(d)$ can be obtained by using the inequality $\sin^2\theta+\Gamma\Omega_l/m_l \le 1+\Gamma\Omega_l/m_l \le 1+2\Gamma\Omega_l \le 1+2\Gamma\max_l\Omega_l$. By defining $\omega = 2\max_l\Omega_l$, we now lower bound (35) as

$$\overline{P}_2(d) \ge (1+\Gamma\omega)^{-d\sum_{l=0}^{L-1}m_l}\frac{1}{\pi}\int_{\theta=0}^{\frac{\pi}{2}} d\theta[\sin^2\theta]^{d\sum_{l=0}^{L-1}m_l} = D(m,d)(1+\Gamma\omega)^{-md} \quad (36)$$

where, as previously defined, $m = \sum_{l=0}^{L-1} m_l$ and

$$D(m,d) = \frac{1}{\pi}\int_{\theta=0}^{\frac{\pi}{2}} d\theta[\sin^2\theta]^{d\sum_{l=0}^{L-1}m_l} = \frac{1}{2\pi}\beta\left(md+\frac{1}{2},\frac{1}{2}\right) \quad (37)$$

where $\beta(p,q) = 2\int_0^{\pi/2} d\theta \sin^{2p-1}\theta\cos^{2q-1}\theta$ is the standard beta integral [19].

Appendix B
Convexity of $D_{\text{lower}}(r_s)$

Upon taking the derivative of (31), we obtain

$$\begin{aligned}\frac{d^2}{dr_s^2}D_{\text{lower}}(r_s) &= 4\epsilon(\ln 2)^2 2^{-2r_s} + 2t(d_{\text{free}})D(m,d_{\text{free}})\epsilon(\ln 2)\\ &\times\left(-2^{-2r_s}md_{\text{free}}\omega(1+\Gamma\omega)^{-md_{\text{free}}-1}\frac{d\Gamma}{dr_s}\right)\\ &-4\epsilon t(d_{\text{free}})D(m,d_{\text{free}})(1+\Gamma\omega)^{-md_{\text{free}}}(\ln 2)^2 2^{-2r_s}\\ &+2\epsilon t(d_{\text{free}})D(m,d_{\text{free}})(\ln 2)2^{-2r_s}\\ &\times\left(-md_{\text{free}}\omega(1+\Gamma\omega)^{-md_{\text{free}}-1}\frac{d\Gamma}{dr_s}\right)+t(d_{\text{free}})\\ &\times D(m,d_{\text{free}})(1-\epsilon 2^{-2r_s})\\ &\times\left(md_{\text{free}}(md_{\text{free}}+1)(1+\Gamma\omega)^{-md_{\text{free}}-2}\omega^2\left(\frac{d\Gamma}{dr_s}\right)^2\right.\\ &\left.-md_{\text{free}}\omega(1+\Gamma\omega)^{-md_{\text{free}}-1}\frac{d^2\Gamma}{dr_s^2}\right) \quad (38)\end{aligned}$$

where $d\Gamma/dr_s$ is given in (32), whose derivative, $d^2\Gamma/dr_s^2$, can be calculated as

$$\begin{aligned}\frac{d^2\Gamma}{dr_s^2} &= -\frac{d\Gamma}{dr_s}\left(\frac{\frac{\Delta\gamma_b}{C_0}}{1+r_s\frac{\Delta\gamma_b}{C_0}}\right)+\frac{\Gamma\frac{\Delta\gamma_b}{C_0}}{\left(1+r_s\frac{\Delta\gamma_b}{C_0}\right)^2}\frac{\Delta\gamma_b}{C_0}\\ &= 2\Gamma\left(\frac{\frac{\Delta\gamma_b}{C_0}}{1+r_s\frac{\Delta\gamma_b}{C_0}}\right)^2 \quad (39)\end{aligned}$$

which is always positive. Upon rearranging (38), by keeping in mind that $t(d_{\text{free}})D(m,d_{\text{free}})(1+\Gamma\omega)^{-md_{\text{free}}} < 1$, we arrive at

$$\begin{aligned}\frac{d^2}{dr_s^2}D_{\text{lower}}(r_s) &= -4\epsilon(\ln 2)2^{-2r_s}t(d_{\text{free}})D(m,d_{\text{free}})md_{\text{free}}\omega\\ &\times(1+\Gamma\omega)^{-md_{\text{free}}-1}\frac{d\Gamma}{dr_s}+4\epsilon(\ln 2)^2 2^{-2r_s}\\ &\times\left(1-t(d_{\text{free}})D(m,d_{\text{free}})(1+\Gamma\omega)^{-md_{\text{free}}}\right)\\ &+(1-\epsilon 2^{-2r_s})(1+\Gamma\omega)^{-md_{\text{free}}-2}t(d_{\text{free}})D(m,d_{\text{free}})\\ &\times md_{\text{free}}\omega\times\left(\frac{\frac{\Delta\gamma_b}{C_0}}{1+r_s\frac{\Delta\gamma_b}{C_0}}\right)^2\\ &\times\left(\omega(md_{\text{free}}+1)\Gamma^2-2(1+\Gamma\omega)\Gamma\right). \quad (40)\end{aligned}$$

Note that the first two terms of (40) are always positive. Now, consider the expression $\omega(md_{\text{free}}+1)\Gamma^2-2(1+\Gamma\omega)\Gamma$ in the third term of (40), which can be simplified as

$$\begin{aligned}&\omega(md_{\text{free}}+1)\Gamma^2-2(1+\Gamma\omega)\Gamma\\ &\quad=(\Gamma\omega(md_{\text{free}}-1)-2)\Gamma\\ &\quad=\left(2\Gamma\max_l\{\Omega_l\}(md_{\text{free}}-1)-2\right)\Gamma\\ &\quad=2\left(\Gamma\max_l\{\Omega_l\}(md_{\text{free}}-1)-1\right)\Gamma. \quad (41)\end{aligned}$$

Since $md_{\text{free}} > 1$ and $\Gamma\max_l\{\Omega_l\} = \overline{\Gamma}_{\max}$ is the maximum average signal-to-interference-plus-noise ratio which we have assumed to be greater than unity (i.e., 0 dB), (41) is always positive. Thus, the third term of (40) is also positive, which proves that $D_{\text{lower}}(r_s)$ is convex.

References

[1] R. L. Pickholtz, L. B. Milstein, and D. L. Schilling, "Spread spectrum for mobile communications," *IEEE Trans. Veh. Technol.*, vol. 40, no. 2, pp. 313–322, May 1991.

[2] A. J. Viterbi, *CDMA: Principles of Spread Spectrum Communication*. Reading, MA: Addison-Wesley, 1995.

[3] M. K. Simon, J. K. Omura, R. A. Scholtz, and B. K. Levitt, *Spread Spectrum Communications Handbook*. New York: McGraw-Hill, 2002.

[4] B. Hochwald and K. Zeger, "Tradeoff between source and channel coding," *IEEE Trans. Inf. Theory*, vol. 43, no. 5, pp. 1412–1424, Sep. 1997.
[5] B. Hochwald, "Tradeoff between source and channel coding on a Gaussian channel," *IEEE Trans. Inf. Theory*, vol. 44, no. 7, pp. 3044–3055, Nov. 1998.
[6] K. H. Li and L. B. Milstein, "On the optimum processing gain of a block-coded direct-sequence spread-spectrum system," *IEEE J. Sel. Areas Commun.*, vol. 7, pp. 618–626, May 1989.
[7] V. V. Veeravalli and A. Mantravadi, "The coding-spreading tradeoff in CDMA systems," *IEEE J. Sel. Areas Commun.*, vol. 20, no. 2, pp. 396–408, Feb. 2002.
[8] Q. Zhao, P. C. Cosman, and L. B. Milstein, "Tradeoffs in source coding, channel coding and spreading in frequency selective Rayleigh-fading channels," *J. VLSI Signal Process.*, vol. 30, no. 1–3, pp. 7–20, Feb. 2002.
[9] ——, "Optimal allocation of bandwidth for source coding, channel coding and spreading in CDMA systems," *IEEE Trans. Commun.*, vol. 52, no. 10, pp. 1797–1808, Oct 2004.
[10] P. Frenger, P. Orten, and T. Ottosson, "Convolutional codes with optimum distance spectrum," *IEEE Commun. Lett.*, vol. 3, no. 11, pp. 317–319, Nov. 1999.
[11] A. Mehes and K. Zeger, "Binary lattice vector quantization with linear block codes and affine index assignments," *IEEE Trans. Inf. Theory*, vol. 44, pp. 79–94, Jan. 1998.
[12] N. Nakagami, "The m-distribution, a general formula for intensity distribution of rapid fading," in *Statistical Methods in Radio Wave Propagation*, W. G. Hoffman, Ed. Oxford, U.K.: Pergamon, 1960, pp. 3–36.
[13] T. Eng and L. B. Milstein, "Coherent DS-CDMA performance in Nakagami multipath fading," *IEEE Trans. Commun.*, vol. 43, no. 2–4, pp. 1134–1143, 1995.
[14] G. P. Efthymoglou, V. A. Aalo, and H. Helmken, "Performance analysis of coherent DS-CDMA systems in a Nakagami multipath fading channel with arbitrary parameters," *IEEE Trans. Veh. Technol.*, vol. 46, no. 2, pp. 289–297, May 1997.
[15] R. Johannesson and K. S. Zigangirov, *Fundamentals of Convolutional Codes*. Piscataway, NJ: IEEE Press, 1999.
[16] A. Gersho and R. M. Gray, *Vector Quantization and Signal Compression*. Norwell, MA: Kluwer, 1992.
[17] E. Erkip, Y. Wang, D. Goodman, Y. Wu, and X. Lu, "Energy efficient coding and transmission," in *Proc. IEEE Veh. Technol. Conf.*, 2001, pp. 1444–1448.
[18] J. W. Craig, "A new simple and exact result for calculating the probability of error for two-dimensional signal constellation," in *Proc. IEEE MILCOM'91*, 1991, pp. 571–575.
[19] M. Abramowitz and I. A. Stegun, Eds., *Handbook of Mathematical Functions*, 9th ed. New York: Dover, 1970.
[20] J. Hagenauer, "Rate-compatible punctured convolutional codes (RCPC codes) and their applications," *IEEE Trans. Commun.*, vol. 36, no. 4, pp. 389–400, Apr. 1988.

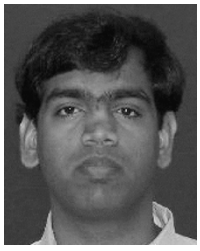

Ramesh Annavajjala (S'03) received the B.Tech. degree in electronics and communication engineering from the National Institute of Technology (NIT), Warangal, India, in May 1998, and the M.S. degree in telecommunications from the Indian Institute of Science, Bangalore, India, in January 2001. Currently, he is working towards the Ph.D. degree at the University of California, San Diego.

From July 1998 to July 1999, he was with CMC R&D Center, Hyderabad, India, and from February 2001 to August 2002, he was a Systems Design Engineer at Synopsys, Inc., Bangalore Center, Wireless and Broadband Communications Group. His research interests lie in the areas of wireless communications, design and analysis of multiple-antenna systems and wideband CDMA systems.

Mr. Annavajjala is a recipient of the Purkayastha/TimeLine Ventures Fellowship Award from 2002 to 2003.

Pamela C. Cosman (S'88–M'93–SM'00) received the B.S. degree (honors) in electrical engineering from the California Institute of Technology, Pasadena, in 1987, and the M.S. and Ph.D. degrees in electrical engineering from Stanford University, Stanford, CA, in 1989 and 1993, respectively.

She was a National Science Foundation (NSF) Postdoctoral Fellow at Stanford University and a Visiting Professor at the University of Minnesota during 1993-1995. In 1995, she joined the faculty of the Department of Electrical and Computer Engineering, University of California, San Diego, where she is currently a Professor and Co-Director of the Center for Wireless Communications. Her research interests are in the areas of image and video compression and processing.

Dr. Cosman is a member of Tau Beta Pi and Sigma Xi. She is the recipient of the ECE Departmental Graduate Teaching Award (1996), a Career Award from the National Science Foundation (1996-1999), and a Powell Faculty Fellowship (1997-1998). She was an Associate Editor of the IEEE COMMUNICATIONS LETTERS (1998-2001), a Guest Editor of the June 2000 Special Issue of the IEEE JOURNAL ON SELECTED AREAS IN COMMUNICATIONS on "Error-Resilient Image and Video Coding," and was the Technical Program Chair of the 1998 Information Theory Workshop in San Diego. She is currently an Associate Editor of the IEEE SIGNAL PROCESSING LETTERS, and a Senior Editor of the IEEE JOURNAL ON SELECTED AREAS IN COMMUNICATIONS. Her web page address is http://www.code.ucsd.edu/cosman/.

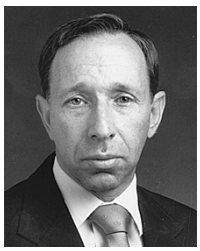

Laurence B. Milstein (S'66–M'68–SM'77–F'85) received the B.E.E. degree from the City College of New York, New York, in 1964, and the M.S. and Ph.D. degrees in electrical engineering from the Polytechnic Institute of Brooklyn, Brooklyn, NY, in 1966 and 1968, respectively.

From 1968 to 1974, he was with the Space and Communications Group, Hughes Aircraft Company, and from 1974 to 1976, he was a member of the Department of Electrical and Systems Engineering, Rensselaer Polytechnic Institute, Troy, NY. Since 1976, he has been with the Department of Electrical and Computer Engineering, University of California at San Diego, La Jolla, where he is a Professor and former Department Chairman, working in the area of digital communication theory with special emphasis on spread-spectrum communication systems. He has also been a consultant to both government and industry in the areas of radar and communications.

Dr. Milstein is a recipient of the 1998 Military Communications Conference Long Term Technical Achievement Award, an Academic Senate 1999 UCSD Distinguished Teaching Award, an IEEE Third Millennium Medal in 2000, the 2000 IEEE Communication Society Armstrong Technical Achievement Award, and the 2002 MILCOM Fred Ellersick Award. He was an Associate Editor for Communication Theory for the IEEE TRANSACTIONS ON COMMUNICATIONS, an Associate Editor for Book Reviews for the IEEE TRANSACTIONS ON INFORMATION THEORY, an Associate Technical Editor for the *IEEE Communications Magazine*, and the Editor-in-Chief of the IEEE JOURNAL ON SELECTED AREAS IN COMMUNICATIONS. He was the Vice President for Technical Affairs in 1990 and 1991 of the IEEE Communications Society, and has been a member of the Board of Governors of both the IEEE Communications Society and the IEEE Information Theory Society. He is a former Chair of the IEEE Fellows Selection Committee, and a former Chair of ComSoc's Strategic Planning Committee.